Title: Verification of the use of GEANT4 and MCNPX Monte Carlo codes for calculations of the depth-dose distributions in water for the proton therapy of eye tumours

Author: Małgorzata Grządziel, Adam Konefał, Wiktor Zipper, Robert Pietrzak, Ewelina Bzymek

Citation style: Grządziel Małgorzata, Konefał Adam, Zipper Wiktor, Pietrzak Robert, Bzymek Ewelina. (2014). Verification of the use of GEANT4 and MCNPX Monte Carlo codes for calculations of the depth-dose distributions in water for the proton therapy of eye tumours. "Nukleonika" (Vol. 59, iss. 2, (2014), s. 61-66), doi 10.2478/nuka-2014-0007

NUKLEONIKA 2014;59(2):61–66
doi: 10.2478/nuka-2014-0007

ORIGINAL PAPER

DE GRUYTER
OPEN

Verification of the use of GEANT4 and MCNPX Monte Carlo codes for calculations of the depth-dose distributions in water for the proton therapy of eye tumours

Małgorzata Grządziel, Adam Konefał, Wiktor Zipper, Robert Pietrzak, Ewelina Bzymek

Abstract. Verification of calculations of the depth-dose distributions in water, using GEANT4 (version of 4.9.3) and MCNPX (version of 2.7.0) Monte Carlo codes, was performed for the scatterer-phantom system used in the dosimetry measurements in the proton therapy of eye tumours. The simulated primary proton beam had the energy spectra distributed according to the Gauss distribution with the cut at energy greater than that related to the maximum of the spectrum. The energy spectra of the primary protons were chosen to get the possibly best agreement between the measured relative depth-dose distributions along the central-axis of the proton beam in a water phantom and that derived from the Monte Carlo calculations separately for the both tested codes. The local depth-dose differences between results from the calculations and the measurements were mostly less than 5% (the mean value of 2.1% and 3.6% for the MCNPX and GEANT4 calculations). In the case of the MCNPX calculations, the best fit to the experimental data was obtained for the spectrum with maximum at 60.8 MeV (more probable energy), FWHM of the spectrum of 0.4 MeV and the energy cut at 60.85 MeV whereas in the GEANT4 calculations more probable energy was 60.5 MeV, FWHM of 0.5 MeV, the energy cut at 60.7 MeV. Thus, one can say that the results obtained by means of the both considered Monte Carlo codes are similar but they are not the same. Therefore the agreement between the calculations and the measurements has to be verified before each application of the MCNPX and GEANT4 codes for the determination of the depth-dose curves for the therapeutic protons.

Key words: depth-doses • GEANT4 • MCNPX • therapeutic protons

M. Grządziel, A. Konefał✉, W. Zipper, R. Pietrzak, E. Bzymek
Department of Nuclear Physics and Its Application, Institute of Physics,
University of Silesia,
4 Uniwersytecka Str., 40-007 Katowice, Poland,
Tel.: +48 32 359 1888, Fax: +48 32 258 8431,
E-mail: akonefal@us.edu.pl

Received: 26 June 2013
Accepted: 16 April 2014

Introduction

The accurate calculations of doses delivered to patients are essential for successful proton therapy. The Monte Carlo computer simulation is considered to be the most accurate method used in these calculations. Its routine clinical application is limited because it needs the appropriately long computation time to get results with a good statistics. Therefore, the treatment planning systems are usually based on simplified methods. However, it is often necessary to make accurate calculations beyond a treatment planning system and the use of the Monte Carlo simulations is the best solution then. The purpose of the presented studies was verification of calculations of the depth-dose distributions in water using GEANT4 and MCNPX Monte Carlo codes for the proton therapy of eye tumours. The calculations were carried out for the real scatterer-phantom system used in the dosimetry measurements in a proton ocular radiotherapy. The first stage of the investigation was the check of agreement of results obtained with the use of the both codes. Finally, the calculated depth-dose distributions in water were compared with those obtained by means of dosimetry measurements. The both Monte Carlo codes are com-

monly used for various calculations in Hadron therapy as well as in classical radiotherapy and in radiation medical physics. GEANT4 and MCNPX codes were applied successfully for calculations of stopping power coefficients and ranges of electrons, protons and alpha particles in liquid water [1, 2], the determination of energy spectra of therapeutic X-rays in water [3] and energy spectra of protons [4], the determination of FWHM and depths of Bragg peak for protons with various energies [5, 6] and LET values for protons and carbon ions [7], calculations of CT images [8–10], a spread-out Bragg peak for a variable-magnetic-field-based energy-selection system [11] and radio-induced DNA damage quantifications [12], etc. There can be also found a lot of papers with applications of GEANT4 and MCNPX codes for purposes of radiation protection of patients and personnel operating medical devices. The examples of applications in the area of radiation protection can be calculations of a radiation field around accelerators [4, 13], estimations of the organ doses in HDR brachytherapy [14] and in proton eye therapy [15], estimations of the alpha doses absorbed during inhalation of short-lived radon progeny [16], the determination of uncertainties in the mean excitation energy of human tissue during proton therapy [17] and optimization of individual patient shielding [18], etc. Comparison of MCNPX and GEANT4 codes in the range of calculations of proton energy depositions for clinical use (CT images) performed by Titt *et al*. [10] are indicative to good agreements between results obtained by both codes. The GEANT4 code was also tested by Cirrone *et al*. [7] for proton dose calculations. However, the Cirrone's test was performed for the simple scatterer-phantom system for protons and carbon ions with energy of 62 AMeV (A – number of nucleons). The presented investigations were carried out for the real scatterer-phantom system used in a proton ocular radiotherapy facility in the Henryk Niewodniczański Institute of Nuclear Physics of the Polish Academy of Sciences in Krakow (Poland), in which the 60 MeV proton beam is applied. The protons are accelerated in the AIC-144 isochronous cyclotron. The main Monte Carlo simulations were carried out using the computers in the Department of Nuclear Physics and Its Applications of the University of Silesia in Katowice (Poland) and the computers of PL-Grid Infrastructure, under the Linux operating system.

Materials and methods

Monte Carlo simulations

GEANT4 in version of 4.9.3 and MCNPX in version of 2.7.0 were used in the simulation programs. The calculations were carried out for the default simulation parameters of the both codes. The simulated source of primary protons was in the shape of a circle with the radius of 9.5 mm. The primary proton spatial distribution was homogeneous in the plane perpendicular to the central-axis of the beam, i.e. to the directions of the proton propagation. The primary proton beam had the energy spectra distributed according to the Gauss distribution with the cut at energy greater than that corresponding to the maximum of the spectrum. The energy spectra was chosen separately for each code to get the possibly best fit to the experimental data, i.e. to the measured relative depth-dose distributions (curves) along the central-axis of the proton beam in a water phantom. In the case of the MCNPX calculations energy of the maximum of the spectrum was 60.8 MeV (more probable energy). FWHM of the spectrum was 0.4 MeV and the energy cut was at 60.85 MeV. In the case of the GEANT4 calculations the best fit to the experimental data was obtained for the spectrum with maximum at 60.5 MeV, the energy cut at 60.7 MeV and FWHM of 0.5 MeV.

The following physical processes were taking into account in the simulation:

- elastic and inelastic interactions, multiple scattering for protons and electrons and additional nuclear reactions for protons;
- photoelectric effect, Compton interaction, gamma conversion and Rayleigh scattering for photons;
- elastic/inelastic scattering and simple capture for neutrons;
- some others of the lower significance, for example, atomic relaxation, the Auger effect, radioactive decay, etc.

The depth-doses were calculated in logic detectors, i.e. in the determined volumes inside a $10 \times 10 \times 10$ cm water phantom. Each logic detector was in the shape of a box of $20 \times 20 \times 0.08$ mm. Wider logic detectors make it possible to get better statistic but it causes a decrease of accuracy of the depth-dose distribution determination, particularly, in the Bragg peak region. The distance between the centres of the neighbouring boxes was 0.1 mm. The simulated scatterer-phantom system is presented in Fig. 1. The geometric details of this system and materials used in its constructions are included in Table 1.

Measurements

Measurements of the depth-dose distributions along the central-axis of the proton beam in a water phantom were performed to verify the results obtained by the Monte Carlo calculations. The scatterer-phantom system applied in the measurements corresponded to the simulated one. The measurements were carried out with the use of the PTW 23343 Markus ionization chamber at the eye therapy room of the Institute of Nuclear Physics of the Polish Academy of Sciences in Krakow [19]. The ionization chamber was shifted from 2 to 30 mm (with the step shorter than 0.1 mm) to get one central-axis depth-dose curve in water. The measurements of the depth-doses were performed according to the recommendation of IAEA TRS-398 [20].

Results

The first stage of the presented investigation was a comparison of the relative depth-dose distributions obtained with the use of MCNPX and GEANT4 codes. The depth-dose distributions were calculated along the central-axis of the considered proton beam in water for the scatterer-phantom system shown in Fig. 1. Additionally, the relative depth-dose distributions were calculated for each scatterer separately for the better comparison.

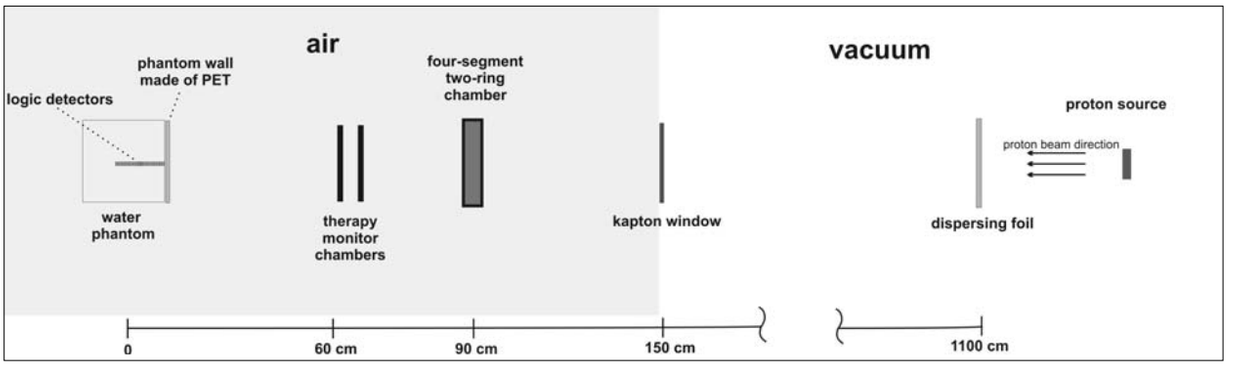

Fig. 1. Scheme of the simulated scatterer-phantom system applied for verification of a depth-dose distributions calculated with the use of GEANT4 and MCNPX codes.

The obtained curves are compared in Fig. 2. The parameters of the calculated curves are included in Table 2.

The Bragg peaks obtained with the use of MCNPX code are slightly shifted (i.e. about 0.1 mm) compared with that derived from the GEANT4 calculations for each considered scatterer with the exception of the ionization chambers where the complete agreement appears. Moreover, the GEANT4 calculations give the 0.1 mm wider Bragg peaks than those calculated with the use of the MCNPX code. In the case of the relative

Table 1. The detailed information about the geometry and materials of the simulated scatterer-phantom system

Simulated object	Thickness along central-axis of beam (cm)	Distance between centre of object and centre of phantom (cm)*	Material and its density (g/cm^3)
Dispersing foil	0.0025	1100	Ta, 16.65
Kapton window	0.003	149	$4C_{22}H_{10}O_5N_2$, 1.42
Aluminium components of four-segment two-ring ionization chamber	0.0008	90.0054 90.6046 92.0046 92.6096	Al, 2.7
Kapton components of four--segment two-ring ionization chamber	0.01	90 90.61 92 92.61	$4C_{22}H_{10}O_5N_2$, 1.42
Air volume of first therapy monitor ionization chamber	0.262	74	N-78%, O-21%, Ar-1%, 0.0012
Carbon components of first therapy monitor ionization chamber	0.001	73.8745 74.1255	C, 2.1
Kapton components of first therapy monitor ionization chamber	0.005	73.8715 73.8745 74.1255 74.1285	$4C_{22}H_{10}O_5N_2$, 1.42
Air volume of second therapy monitor ionization chamber	0.262	61	N-78%, O-21%, Ar-1%, 0.0012
Carbon components of second therapy monitor ionization chamber	0.001	68.8745 69.1255	C, 2.1
Kapton components of second therapy monitor ionization chamber	0.005	68.8715 68.8745 69.1255 69.1285	$4C_{22}H_{10}O_5N_2$, 1.42
PET (polyethylene terephthalate) phantom wall	0.054	5.1	$3C_{10}H_8O_4$, 1.27
Water phantom	10	0	H_2O, 1.00

*The distances included in column 3 were used in the calculations. In the real system the precision of some distances is of course unreachable, because of many reasons like the thermal effect, for example. It gives its contribution to the differences between the calculated depth-dose distributions and the measured one.

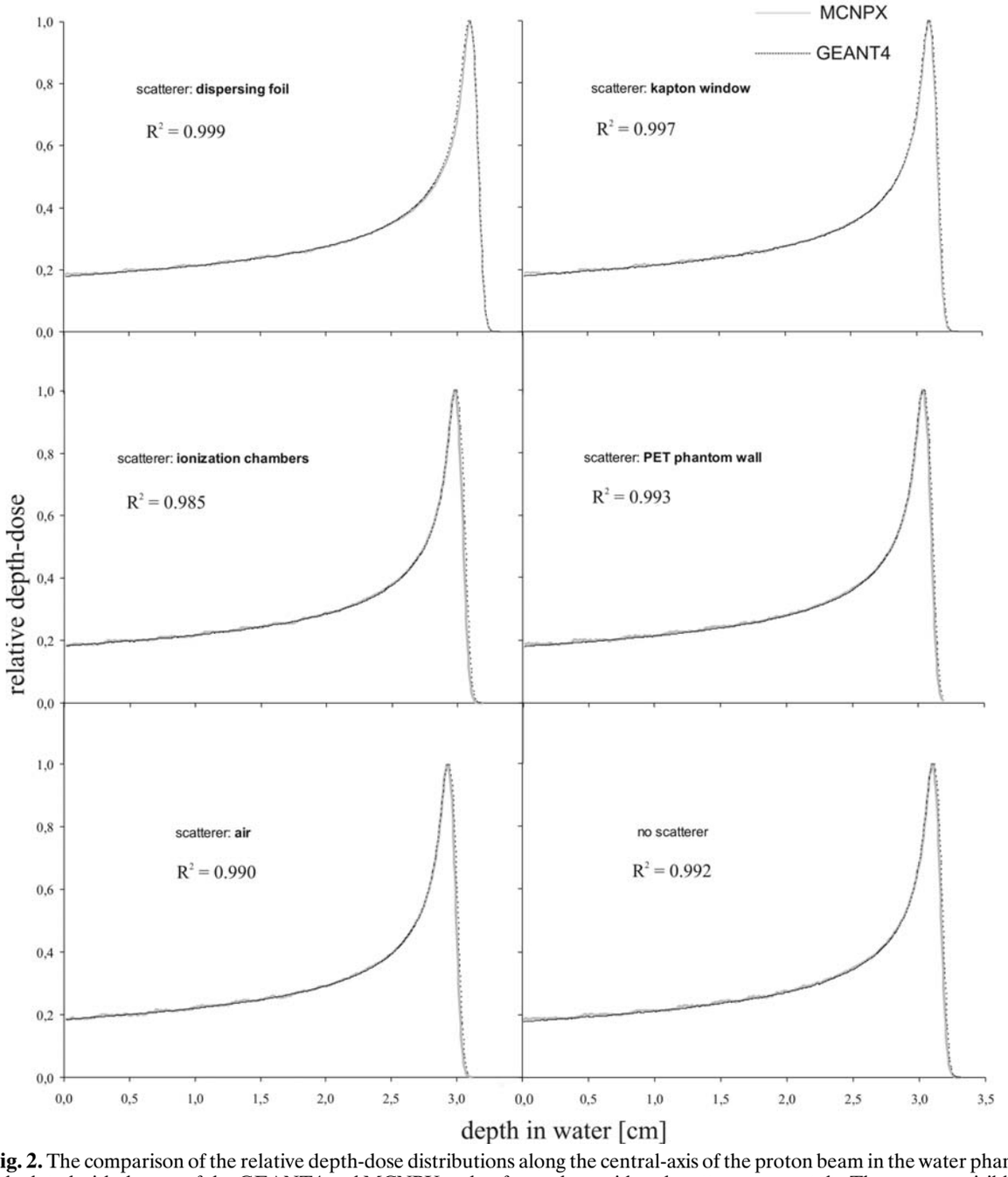

Fig. 2. The comparison of the relative depth-dose distributions along the central-axis of the proton beam in the water phantom, calculated with the use of the GEANT4 and MCNPX codes, for each considered scatterer separately. There are no visible differences between the curves calculated using the GEANT4 code and the MCNPX one. The values of a square of the Pearson correlation coefficients R^2 for the relative depth-dose curves calculated with the use of GEANT4 and MCNPX are close to 1 for each scatterer. It is indicative to a good agreement between calculations performed by means of the both codes.

depth-dose curves calculated applying the MCNPX code the ratio of the minimum dose to the maximum dose D_{min}/D_{max} is equal to 0.19 for each considered scatterer contrary to the GEANT4 calculations where the values of D_{min}/D_{max} range from 0.17 to 0.18. However, D_{min}/D_{max} is equal to 0.19 for the both codes for the full scattering system.

In the second stage of the presented study the obtained relative depth-dose curves for the full scatterer--phantom system were compared with those from the experiment. The comparison of the calculations and the measurements is presented in Figs. 3, 4 and Table 3. The square of the Pearson correlation coefficient was also determined for the calculated and measured relative depth-dose curves presented in Fig. 3 to check the agreement between the curves from the Monte Carlo calculations and from the measurements. There is a good correlation between the data obtained with the use of the MCNPX and GEANT4 codes ($R^2_{MCNPX\_GEANT4}$ = 0.999) as well as between the calculated curves and the measured curve ($R^2_{MCNPX\_Meas}$ = 0.997, $R^2_{GEANT4\_Meas}$ = 0.996). The local differences between the measured and calculated relative depth-doses are less than 5% in most cases (see Fig. 4) for the uncertainty in the Monte Carlo calculations (statistical fluctuations) less than 4% and for the measuring error of about 1%. The mean value of the local differences is equal to 2.1% and 3.6%

Table 2. The parameters (D_{min}/D_{max}, FWHM of Bragg peak, the depth of the maximum dose) describing the relative depth-dose distributions along the central-axis of the beam in the water phantom, obtained for the proton beam after passing through vacuum. Air, the dispersing foil, the Kapton window, the therapy monitor chambers, the PET phantom wall and the full scattering system consisting of all mentioned scatterers

Scatterer	D_{min}/D_{max}*		FWHM of Bragg peak (mm)		Depth of maximum dose (mm)	
	GEANT4	MCNPX	GEANT4	MCNPX	GEANT4	MCNPX
Vacuum	0.17	0.19	3.1	3.0	31.1	31.0
Air	0.18	0.19	3.1	3.0	29.4	29.3
Dispersing foil	0.18	0.19	3.1	3.0	30.9	31.0
Kapton window	0.18	0.19	3.1	3.0	31.0	30.9
PET phantom wall	0.18	0.19	3.1	3.0	30.4	30.3
Ionization chambers	0.18	0.19	3.1	3.0	29.8	29.8
Full scattering system	0.19	0.19	3.1	3.0	27.3	27.4

*D_{min} – the minimum dose, i.e. the dose registered in the first bin adjacent to the surface of water. D_{max} – the dose at the depth of the Bragg peak.

Table 3. The comparison of the parameters of the measured and calculated relative depth-dose distributions along the central-axis of the proton beam in water for the full scattering system

	D_{min}/D_{max}	FWHM of Bragg peak (mm)	Depth of maximum dose (mm)
Measurements	0.20	2.8	28.1
MCNPX	0.19	3.0	28.1
GEANT4	0.19	3.1	27.9

The PET phantom wall was converted into the equivalent water layer.

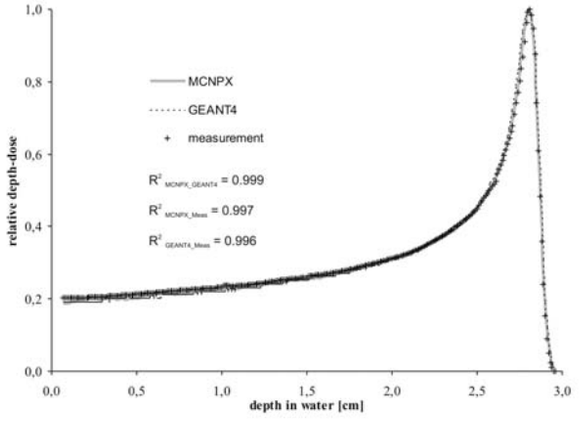

Fig. 3. The relative depth-dose distributions along the central-axis of the beam in the water phantom for the considered proton beam, for the full scatterer-phantom system. The curves were obtained with the use of the Monte Carlo calculations based on the GEANT4 and MCNPX codes as well as on the measurements performed by the Markus ionization chamber. The presented curves were obtained after the conversion of the PET phantom wall into the equivalent water layer. $R^2_{MCNPX\_GEANT4}$ – a square of the Pearson correlation coefficient for the curves calculated with the use of the MCNPX code and the GEANT4 code, $R^2_{MCNPX\_Meas}$ – a square of the Pearson correlation coefficient for the curve calculated applying the MCNPX code and the measured curve, $R^2_{GEANT4\_Meas}$ – a square of the Pearson correlation coefficient for the curve calculated using the GEANT4 code and the curve from the measurements.

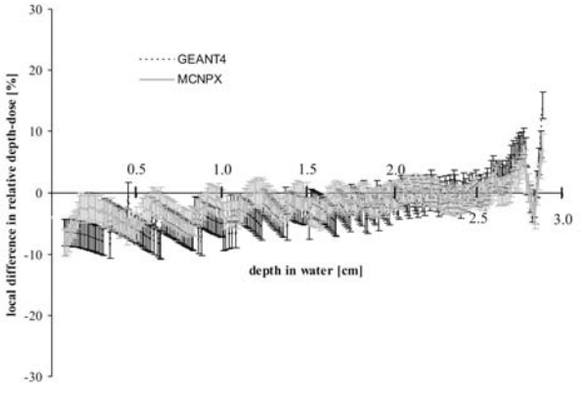

Fig. 4. The local differences between the relative central-axis beam depth-doses obtained with the use of the Monte Carlo calculations and the measurements in the water phantom.

for the MCNPX and GEANT4 calculations, respectively. The maximum local differences do not exceed 10%. The greatest differences appear in the range of depths with the largest gradient of the depth-dose, i.e. in the region of the Bragg peak. It is caused by the fact that in this largest gradient region the active volume of the ionization chamber applied in the measurements contains the region with depth-doses differing significantly from each other. Thus, the readings of the ionization chamber are the mean depth-dose in the active volume whereas the logic detectors were several times thinner (in the direction of the beam propagation) than the active volume of the ionization chamber, to get the possibly precise representation of the depth-dose curves.

Discussion and conclusions

The presented investigations were performed for the chosen materials (seven materials composed of six elements). The both considered Monte Carlo codes give the similar results for each considered scatter as well as for the full scattering system. However, it is worth noticing that the primary proton beam in the MCNPX calculations had the energy spectrum (more probable energy at 60.8 MeV, FWHM of 0.4 MV, energy

cut at 60.85 MeV) somewhat different from that in the GEANT4 calculations (more probable energy at 60.5 MeV, FWHM of 0.5 MV, energy cut at 60.7 MeV). Such energy spectra give the best agreement between the measured relative depth-dose curves and those calculated with the use of the MCNPX/GEANT4 codes. The optimal spectra of the primary proton beam for each code were obtained in series of the trial simulations. The same spectra for the both codes did not give the best fit to the experimental data. The observed overestimation of depth-doses in the MCNPX calculations (greater energy of the starting proton beams) compared to the GEANT4 code is caused by various models used in estimations of the angular deflection of protons. In MCNPX algorithms a small-angle Coulomb scattering is based on a theory presented by Rossi [21], whereas a modified Highland–Lynch–Dahl formula [22] is applied in GEANT4 in calculations of the angular distribution of protons. The relatively small differences between the calculated depth-dose distributions and the measured one are indicative that GEANT4 as well as MCNPX can be applied for calculations in the dosimetry in a proton ocular radiotherapy. However, one can say that the results obtained by means of the both considered Monte Carlo codes are similar but they are not the same. Therefore the agreement between the calculations and the measurements has to be verified before each application of the MCNPX and GEANT4 codes.

Acknowledgments. Authors of this paper are very grateful to Teresa Cywicka-Jakiel from The Henryk Niewodniczański Institute of Nuclear Physics of the Polish Academy of Sciences in Kraków (Poland) for preparation of the experimental data used in the presented investigations. This research was supported in part by PL-Grid Infrastructure.

References

1. Francis, Z., Incerti, S., Karamitros, M., Tran, H. N., & Villagrasa, C. (2011). Stopping power and ranges of electrons, protons and alpha particles in liquid water using the Geant4-DNA package. *Nucl. Instrum. Meth. Phys. Res. B*, *269*, 2307–2311.
2. Garcia-Molina, R., Abril, I., De Vera, P., & Pau, H. (2013). Comments on recent measurements of the stopping power of liquid water. *Nucl. Instrum. Meth. Phys. Res. B*, *299*, 51–53.
3. Konefał, A., Orlef, A., & Maniakowski, Z. (2010). Influence of the radiation field size and the depth in irradiated medium on energy spectra of the 6 MV X-ray beams from medical linac. *Pol. J. Environ. Stud.*, *1*, 115–118.
4. Ottaviano, G., Picardi, L., Pillon, M., Ronsivalle, C., Sandri, S. (2014). The radiation fields around a proton therapy facility: A comparison of Monte Carlo simulations. *Rad. Phys. Chem.*, *95*, 236–239.
5. Jia, X., Schümann, J., Paganetti, H., & Jiang, S. B. (2012). GPU-based fast Monte Carlo dose calculation for proton therapy. *Phys. Med. Biol., 57*(23), 7783–7797.
6. Konefał, A., Szaflik, P., & Zipper, W. (2010). Influence of the energy spectrum and the spatial spread of the proton beams used in the eye tumor treatment on the depth-dose characteristics. *Nukleonika*, *55*(3), 313–316.
7. Cirrone, G. A. P., Cuttone, G., Mazzaglia, S. E., Romano, F., Sardina, D., Agodi, C., Attili, A., Blancato, A. A., De Napoli, M., Di Rosa, F., Kaitaniemi, P., Marchetto, F., Petrovic, I., Ristic-Fira, A., Shin, J., Tarnavsky, N., Tropea, S., & Zacharatou, C. (2011). Hadrontherapy: a Geant4-based tool for proton/ion-therapy studies. *Prog. Nucl. Sci. Technol.*, *2*, 207–212.
8. Lee, C. C., Lee, Y. J., Tung, C. J., Cheng, H. W., & Chao, T. C. (2014). MCNPX simulation of photon dose distribution in homogeneous and CT phantoms. *Rad. Phys. Chem.*, *95*, 302–304.
9. Sadrozinski, H. F., Johnson, R. P., MacAfee, S., Plumb, A., Steinberg, D., Zatserklyaniy, A., Bashkirov, V. A., Hurley, R. F., & Schulte, R. W. (2013). Development of a head scanner for proton CT. *Nucl. Instrum. Meth. Phys. Res. A*, *699*, 205–210.
10. Titt, U., Bednarz, B., & Paganetti, H. (2012). Comparison of MCNPX and Geant4 proton energy deposition predictions for clinical use. *Phys. Med. Biol.*, *57*, 6381–6393.
11. Kim, D. H., Suh, T. S., Kang, Y. N., Yoo, S. H., Pae, K. H., Shin, D., & Lee, S. B. (2013). Parametric study of a variable-magnetic-field-based energy-selection system for generating a spread-out Bragg peak with a laser-accelerated proton beam. *J. Kor. Phys. Soc.*, *62*(1), 59–66.
12. Francis, Z. (2013). Molecular scale simulation of ionizing particles tracks for radiobiology and Hadron-therapy studies. *Adv. Quan. Chem.*, *65*, 79–110.
13. Konefał, A., Polaczek-Grelik, K., Orlef, A., Maniakowski, Z., & Zipper, W. (2006). Background neutron radiation in the vicinity of Varian Clinac-2300 medical accelerator working in the 20 MV mode. *Pol. J. Environ. Stud.*, *15*(4A), 177–180.
14. Candela-Juan, C., Perez-Calatayud, J., Ballester, F., & Rivard, M. J. (2013). Calculated organ doses using Monte Carlo simulations in a reference male phantom undergoing HDR brachytherapy applied to localized prostate carcinoma. *Med. Phys.*, *40*(3), art. No. 033901.
15. Stolarczyk, L., Olko, P., Cywicka-Jakiel, T., Ptaszkiewicz, M., Swakoń, J., Dulny, B., Horwacik, T., Obryk, B., & Waligórski, M. P. R. (2010). Assessment of undesirable dose to eye-melanoma patients after proton radiotherapy. *Radiat. Meas.*, *45*, 1441–1444.
16. Nikezic, D., Haque, A. K. M. M., & Yu, K. N. (2002). Absorbed dose delivered by alpha particles calculated in cylindrical geometry. *J. Environ. Radioact.*, *60*, 293–305.
17. Besemer, A., Paganetti, H., & Bednarz. B. (2013). The clinical impact of uncertainties in the mean excitation energy of human tissue during proton therapy. *Phys. Med. Biol.*, *58*(4), 887–902.
18. Cywicka-Jakiel, T., Stolarczyk, L., Swakoń, J., Olko, P., & Waligórski, M. P. R. (2010). Individual patient shielding for a proton eye therapy facility. *Radiat. Meas.*, *45*, 1127–1129.
19. Swakoń, J., Olko, P., Adamczyk, D., Cywicka-Jakiel, T., Dabrowska, J., Dulny, B., Grzanka, L., Horwacik, T., Kajdrowicz, T., Michalec, B., Nowaka, T., Ptaszkiewicz, M., Sowa, U., Stolarczyk, L., Waligorski, M. P. R. (2010). Facility for proton radiotherapy of eye cancer at IFJ PAN in Krakow. *Radiat. Meas.*, *45*, 1469–1471.
20. Physics Reference Manual, May 2007.
21. International Atomic Energy Agency. (2000). *Absorbed dose determination in external beam radiotherapy: An international code of practice for dosimetry based on standards of absorbed dose to water*. Vienna: IAEA. (TRS-398).
22. MCNPX User's Manual, April 2002.
23. Park, Y. S., Kim, J. H., Hong, G. B., Jung, I. S., & Yang, T. K. (2011). Proton beam energy determination using a device for range measurement of an accelerated high energy ion beam. *J. Kor. Phys. Soc.*, *59*(22), 679–685.